Comparative Visualization of Two-Dimensional Flow Data Using Moment Invariants

author1, author2

affiliation1
affiliation2
Email: {author1,author2}@affiliation

Abstract

The analysis of time-dependent data is often guided by the question of how dominant structures develop over time. It is important to understand how patterns or structures identified for one time step evolve over time, by changing or moving in the domain. To gain insight into such evolving structural change it is crucial to effectively compare different time steps.

This paper proposes a comparison method for two-dimensional flow fields. The method is based on a feature description using invariant moments. The specific strength of these moments is their invariance under scaling and rotation, thus facilitating an identification of features even if they occur at other positions, with changed orientation, and variation in size. In addition the moments themselves can be used to define a similarity measure.

To evaluate the significance of this concept it has been applied to wind speed data from meteorological simulations.

1 Introduction

The comparison of data is important in various contexts. Examples are the evaluation of numerical methods used for simulations where results from simulations are compared to experimental measurements. Visualization methods can be evaluated by a comparison of different visualization methods using the same data set. A comparison of different time steps of an experiment or a simulation is valuable for understanding the temporal development of structures. Common comparative visualization methods can basically be divided in three different classes [12]: image level, data level and feature level comparison. Image level methods first generate images from the relevant data sets independently. These images are compared either by a human observer or by image analysis methods. A simple way is to use difference images that compare the images pixel by pixel. This method is limited to image data sets where an approximate one-to-one correspondence between pixels exists and similar view parameters for the image generation are used. Data level methods perform the comparison on the basis of the data and finally visualize the result. The main challenge is to find an appropriate dissimilarity measure for data comparison [7, 8].

Comparisons with feature level methods are not directly based on the data but on extracted features. This approach is much more flexible than image or data level methods. For flow analysis there are many interesting feature definitions ranging from topology to vortex core lines, see [9] for an overview, from which the user can choose features of interest. The main challenge is to find an appropriate feature description to be used as a similarity measure. Methods building on the comparison of streamlines were proposed in [6, 12]. Originally these methods have been developed to compare simulation, visualization or feature extraction methods in terms of uncertainty. The comparison of streamlines is restricted to a few carefully chosen sets of streamline pairs. The method is too rigid to consider more general flow structures as complex flow patterns. In [11, 1] systems have been presented that support appropriate views for comparative visualization. Recently, a method for the comparison of nasal airflows has been described [4]; this method uses a combination of data comparison with a certain metric applied to special flow probes in a virtual environment.

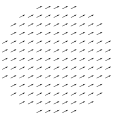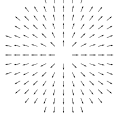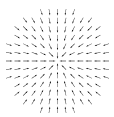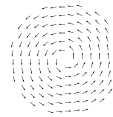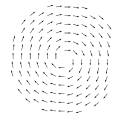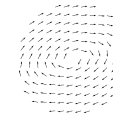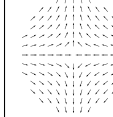For all these methods first a correspondence

homogeneous flow	source / divergence	sink / convergence	counter-clockwise rotation	clockwise rotation	compressed rotation	saddle
$\Psi_1 = 0$	$\Psi_1 = \frac{2}{3\sqrt{\pi}}$	$\Psi_1 = -\frac{2}{3\sqrt{\pi}}$	$\Psi_1 = i\,\frac{2}{3\sqrt{\pi}}$	$\Psi_1 = -i\,\frac{2}{3\sqrt{\pi}}$	$\Psi_1 \approx -i\,0.1677$	$\Psi_1 = 0$
$\Psi_{2,3,4,5} = 0$	$\Psi_{2,3,4,5} = 0$	$\Psi_{2,3,4,5} = 0$	$\Psi_{2,3,4,5} = 0$	$\Psi_{2,3,4,5} = 0$	$\Psi_{2,3,4,5} = 0$	$\Psi_{2,3,4,5} = 0$

Figure 1: Invariant moment values for prototypical linear flow features. Second-order moments ($\Psi_{2,3,4,5}$) are zero due to linearity. For other, general non-linear features second-order moments are non-zero.

from one image to another or from one data set to another or one feature to another has to be defined before being able to apply the distance metrics. Especially for time varying data sets this can be a challenging task. Features might have moved, are scaled or rotated yielding different feature descriptors. Applying statistical analyses might result in some valuable similarity information, but without providing the necessary spatial context. Thus, one should expect certain characteristics of a practically useable comparative visualization tool for time-dependent data: support of an easy interactive feature definition; provision of feature descriptors being invariant to translation, scaling and rotation; provision of feature descriptors that can immediately be used as a similarity measure; fast response to new feature queries making an interactive exploration possible.

Recently *flow moment invariants* have been introduced in [10] following the idea of invariant moments as used for shape recognition. These moments represent characteristics of a two-dimensional (2D) flow field independent of orientation and scale. Flow features correspond to a specific set of invariant moments, which can be defined interactively by brushing regions of interest in one time-step. Thus, invariant moments for scalar and flow fields meet all the desired characteristics of a comparative visualization tool as mentioned above, and serve as a good basis for feature-based data comparison. This paper proposes two different approaches to use invariant moments to reach this goal, applying different similarity metrics.

The paper is structured as follows: first, we provide an overview of flow moment invariants, explaining the definitions and the generation of a *moment pyramid*. Second, we show how these methods can be utilized in the context of comparative visualization. The two methods of interactive pattern comparison and the comparison of moment pyramids are explained. While the first method is suitable for the comparison of all kinds of 2D flow fields, the latter method turns out to be useful especially for the comparison of different time steps in time-varying data.

2 Flow Moment Invariants

2.1 Definitions

Moment invariants have originally been defined for image data. *Moments* are a statistical measure often applied to images to analyze their geometric features. This is commonly an early part of the *classification* process. Originally, *moment invariants* were developed by Hu [5] in the early 1960s. His version was proven to be redundant and incomplete by Flusser [3]. Based upon Flusser's independent and complete set of *moment invariants* flow moment invariants were defined in [10].

Moment invariants represent characteristic values of a geometric structure being invariant to its position, scale, and orientation. In terms of image data, they are often used for text recognition. The idea of flow moment invariants is to store this characteristic information for flow patterns. This is neither possible using the common scalar moment invariants, nor using its component-wise extension to higher dimensions (i.e., moment invariants for color images). This is due to the fact that flow data is correlated to the given domain while image data is not. Details and further explanations can be found in [10]. In this context normalized complex

moments for flows have been defined as follows:

Definition 1 *Let a flow vector pattern* $f : \mathbb{R}^2 \to \mathbb{C} \cong \mathbb{R}^2$ *be a map from* $\mathbb{R}^2$ *with* $f \neq 0$ *in a compact subset* $G \subseteq \mathbb{R}^2$. *Further, let* $p, q \in \mathbb{N}$ *and* $i = \sqrt{-1} \in \mathbb{C}$. *The **normalized complex central flow moments** of order* $(p + q)$ *are defined as*

$$c_{pq} = \frac{1}{v^{\gamma}} \int\limits_{-\infty}^{\infty} \int\limits_{-\infty}^{\infty} (\hat{x} + i\hat{y})^p (\hat{x} - i\hat{y})^q f(x,y) dx dy$$

(1)

with $v = \int_G 1\, dx dy$, $\hat{x} = (x - \bar{x})$, $\hat{y} = (y - \bar{y})$, *and* $\gamma = \frac{p+q+2}{2}$ *(for domain scale invariance).*

With these normalized complex moments for flows, flow moment invariants can be constructed. A basis for flow moment invariants of order 1 and 2 has also been presented in [10]:

$$\begin{aligned}
\Psi_1 &= c_{01}, \\
\Psi_2 &= c_{00}c_{02}, \\
\Psi_3 &= c_{11}c_{02}, \\
\Psi_4 &= c_{10}c_{02}^2, \\
\Psi_5 &= c_{20}c_{02}^3.
\end{aligned}$$

(2)

Each complex value represents an independent characteristic of the analyzed pattern. The values of the Ψs for any given pattern equal the values for any rotated or scaled version of this pattern. This enables a recognition of flow patterns regardless of orientation and scale.

2.2 Moment Pyramid

The presented moment values can be computed for any possible pattern in the data set. Since the moments are defined similarly to the convolution operator, all complex moments c_{ij} can be computed by the application of the well-known convolution operator with the corresponding moment basis functions and a subsequent normalization (see [10]). The convolution is computed for all discrete radii resulting in a *moment pyramid*. Since the convolution operation increases continuity by one degree, small perturbations in the radii between these discrete positions tend to have only limited effects. Similarly to [10] we decided to homogenize the vector magnitudes of the field and store the magnitude information separately as a scalar field to be able to find patterns that are similar in direction. A further exclusion of the patterns with different vector magnitudes can easily be attached

using the previously removed scalar information.

For each scale of the filter masks correlations are performed, each resulting in a field on a two-dimensional domain containing the invariant moments $\Psi_{1\ldots5}$. These fields become smaller for increasing scale of the filter masks, since we decided to omit the border region in our implementation. Thus, the resulting collection of moment fields is called moment pyramid. A moment pyramid provides a discretized description of all vector patterns of an underlying field at each position. The scale of the pattern corresponds to its (height) level in the pyramid. The position of a pattern (center) in the original data is equivalent to its planar coordinates at each specific scale level of the pyramid, see Figure 2. Thus, each data element of the pyramid represents a special feature space vector ($\Psi_{1,\ldots,5}$) describing the underlying patterns of the flow vector field.
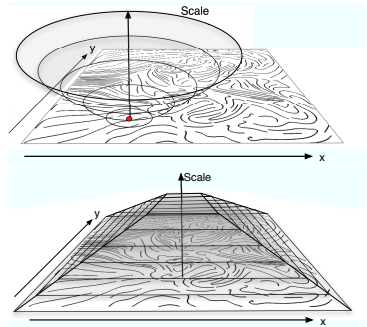

Figure 2: Illustration of a moment pyramid. Moments are computed for varying pattern sizes. Starting with a minimum pattern size of 5×5 the moments are computed for the maximum possible pattern size (limited by the size of the flow field). Storing the moment values for each scale and position results in a pyramid structure.

2.3 Implementation

The computation of the moment invariants is done in a preprocessing step. Convolutions of the flow vector field with the moment invariant basis functions are performed. Regarding accuracy, there are only small discretization errors resulting from the fact that moment invariants are assumed to be on

a circular domain. However, a completely circular domain can never be achieved for discrete data defined on a mesh. Nevertheless, the degree of continuity of the field is increased by the application of a convolution operation. The complete computation effort for this preprocessing is generally on the order of a few minutes. This is about the same effort as for a proper recognition of only one single (general) pattern with the related method of Ebling and Scheuermann [2]. The moment pyramid is further indexed so that patterns can be recognized in an efficient manner. The actual pattern recognitions are finally performed by a simple look-up operation of the moment values in the pyramid (generally requiring a few milliseconds), see [10] for more details.

3 Comparative Visualization of Time-varying Data

We propose two methods for the analysis of time-varying flow data. The comparison is based on features, especially on spatial flow structures. However, there is no focus on special structures (like sources, sinks saddles, etc.) but on the observed general flow behavior. Information regarding the flow structure in differently sized circular areas is stored in a feature vector: the flow moment invariants (see section 2.1). To cover the whole field the feature vectors are stored in a so-called moment pyramid (as explained in section 2.2).

The definition of a suitable metric for the comparison of moment invariants is a key element.

3.1 Difference Metrics

For all subsequent definitions let the flow moment invariant for a pattern P be given by $\Psi_{1,...,5}^P$ and for a second pattern Q by $\Psi_{1,...,5}^Q$. P and Q shall be compared.

Definition 2 *The **first order absolute distance** d_1 of the two patterns P and Q is defined as*

$$d_1 = \left| \Psi_1^Q - \Psi_1^P \right|.$$

*The **second order absolute distance** d_2 is defined as*

$$d_2 = \sum_{i=2}^{5} \left| \Psi_i^Q - \Psi_i^P \right|.$$

*The **complete absolute distance** d_c is defined as*

$$d_c = d_1 + d_2 = \sum_{i=1}^{5} \left| \Psi_i^Q - \Psi_i^P \right|.$$

The absolute distances are defined according to the common distance metric of complex numbers. For the second order moment invariants we compute the sum of all second order distances. The complete absolute distance is a combination of the first and second order. The terms might also be normalized, but there is no need to normalize. In the following, a definition for a relative deviation is given.

Definition 3 *The **complete relative deviation** δ of the two patterns is defined as*

$$\delta = \max \left(\left\{ i \in \{1, ..., 5\} \left| \frac{2|\Psi_i^Q - \Psi_i^P|}{|\Psi_i^P| + |\Psi_i^Q|} \right| \right\} \right).$$

Using this metric, changes in pattern structure can be observed relatively. This formula unfortunately becomes singular when comparing two completely homogeneous structures or perfect saddles, yielding zero in the denominator.

Both metrics indicate the similarity of the underlying structures. The lower the distance (deviation) is, the higher is the similarity of the two compared patterns. The highest degree of similarity is obtained for patterns with equal moment invariants having zero distance (and deviation).

3.2 Interactive Pattern Comparison

In this section an approach for a *feature-based data comparison* is presented. The idea is to generate visualizations of multiple data sets next to each other and use the pattern recognition to highlight similar features. This can be especially useful for the comparative visualization of neighboring time steps from time-dependent flow data. A pattern of interest is chosen by the user by selecting an arbitrary circular region in the spatial domain of a specific time step. The moment pyramid is addressed using the mentioned index. For the comparison of the query pattern moment invariants with the elements in the pyramid, the complete relative deviation metric is used. The desired maximum deviation is chosen by the user, for example $\delta = 3\%$. This means that positions in the moment pyramid where all moment value components $\Psi_{1,...,5}$ vary up to 3% from

the moment components of the pattern of interest are marked. The position in the moment pyramid directly maps to the position and scale in the original field, meaning the pattern recognition returns all positions and corresponding scales of similar flow structures of any time step of the time-varying data. Another important point to mention is that the moment field is a discrete representation of an at least $\mathbb{C}^1$-continuous field. This is due to the fact that it has been obtained by the convolution operator. It is natural to find many similar values in a specific region. However, visualizing all results yields clutter, as there are certain areas where values are similar in the direct neighborhood. Thus, when results are in the immediate spatial neighborhood of each other, only the most similar result are visualized. This increases the clarity of the visualization.

3.3   Moment Pyramid Comparison

The idea of the *flow moment comparison* is similar to the *pyramid comparison* for image data. The *moment pyramid* spans a scale space, similar to the *Gauss pyramid* known from image processing. Subtracting a second pyramid element-wise from the original one yields a *difference pyramid*. For the comparison the metrics defined above are used: the first order, the second order, and the complete absolute distance as well as the complete relative distance.

The distances d_1, d_2, and d_c are calculated for each element of two given moment pyramids. One obtains a scalar-valued difference pyramid for each applied metric. The visualization of the values of a certain pyramid level indicates the similarity of two flow vector fields with respect to structures of a certain size. This means a low pyramid level indicates changes of small structures (high-frequency changes), while a higher pyramid level indicates changes in large structures (low-frequency changes).

4   Results

To illustrate how the presented methods work in practice, the flow data set from Hurricane Isabel, generated in 2003, has been chosen. The pattern comparison was performed for a 2D layer at a height of 3150m, for the first five hours of the data

set, before the hurricane hits the continent.

4.1   Interactive Pattern Comparison

The pattern comparison method can, for example, be used to track patterns over time. Figure 3 shows three different patterns being tracked over five time steps each. The relative deviation was chosen as $\delta = 3\%$ for all pattern searches. The first pattern shown on the left side is a mostly homogenuous flow diverging at one side. In the first time step, the pattern appears once between the two circulations and the saddle point. In time step two, the pattern changed its position towards the vanishing saddle. It is still similar enough to be tracked within the 3% similarity tolerance. Time step three shows the tracked pattern in light-gray, indicating that the pattern has changed its shape being almost outside the similarity tolerance. However, a new pattern of this kind is developing again at a position close to the position in the first time step. This pattern remains until time step five (the last analyzed time step). During the final time step, more patterns of this kind can be observed in the vicinity of the large hurricane turbulence.

The second pattern we decided to track over the same time steps is a saddle (see Figure 3 in the middle). In this case, no other similar structures can be observed, as the additional saddle emerging in time step five is not in the similarity tolerance (3% relative deviation) of the tracked pattern. It is interesting to observe that this pattern remains mainly at the same position close to the coast. It becomes a somewhat larger in time step two, but reduces its size again in the following steps.

The third pattern (Figure 3 on the right side) indicated a perfect example why this method is more revealing than a pure visualization with streamlines. The pattern is also quite homogeneous, with a divergence on one side (towards the coast). It is moving somewhat, but is present in the northern coast region in all five time steps. The pattern is also detected in time steps four and five. In time step four, one would not have succeeded in finding this pattern, as the streamlines do not fully reveal it due to its reduced size. Again, no other similar pattern is appearing.
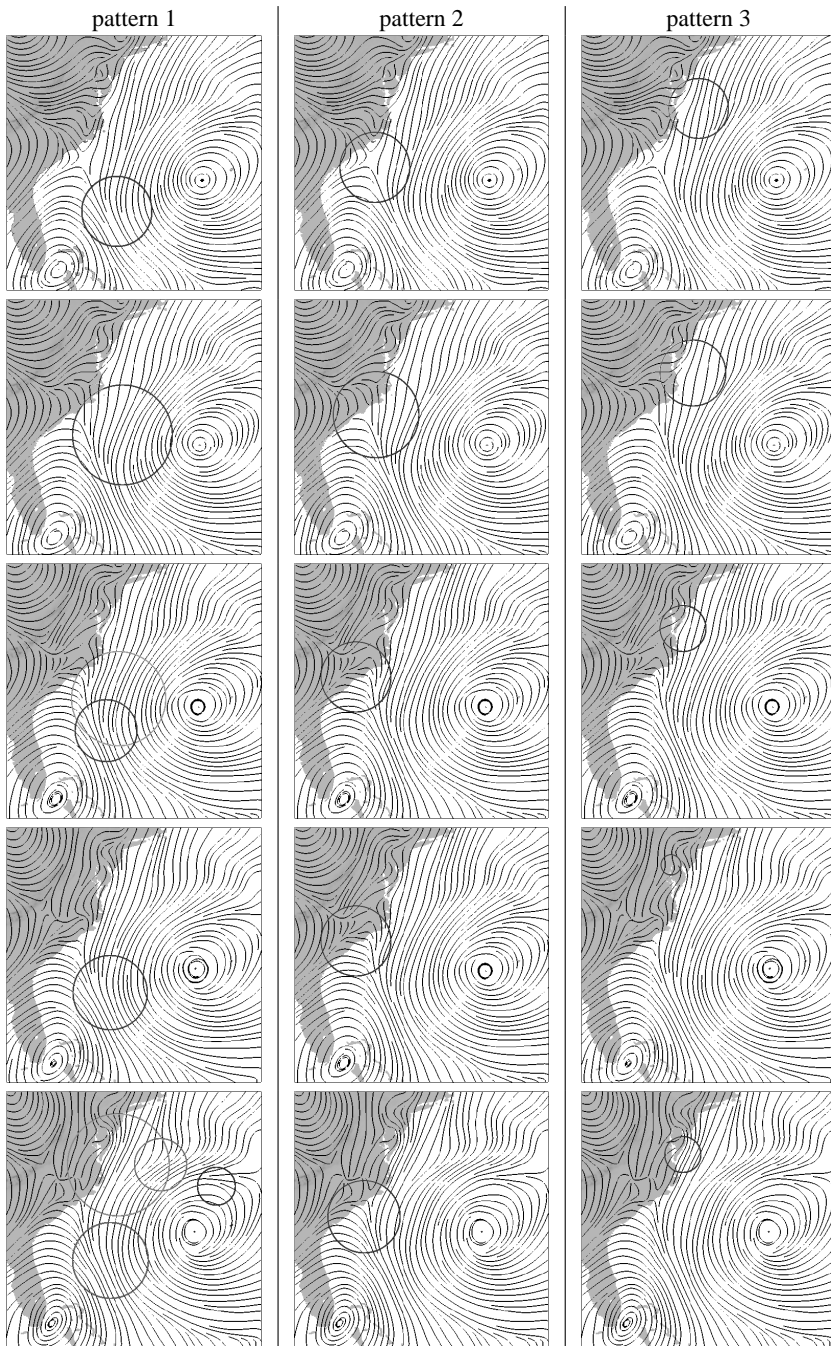
Figure 3: Interactive pattern recognition for the first five hours of a flow simulation (Hurricane Isabel at 3150 meters height): three patterns are selected from a slice at an early time step. The patterns, which stay similar, can be tracked over time.

4.2 Moment Pyramid Comparison

In the following the pyramid comparison is shown for three different metrics: the complete distance, the first order distance and the second order distance (see Figure 4.).
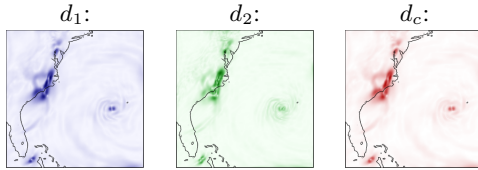

Figure 4: Moment pyramid (level one) comparison between the first and second time step of the Hurricane Isabel data (3150m height) for three different distance definitions.

The distance values are visualizing the movement of topologically and structurally important features. The movement of the saddle (see Figure 3 on the left side) can be seen clearly in this visualization, for first order, second order and combined moment distances. The movement of the center regions can also be observed. More examples for this visualization are presented in Figure 5.

For these visualizations, different pyramid levels have been analyzed. The total pyramid size is 120 layers for the presented data. Layer 60 is a medium layer. The moment distance at this level indicates changes of a medium or low frequency. The distances at such a level might be of value to analyze the future development of the storm. For example, the time step distance $3 - 4$ shows that two major regions of activity are about to join. The resulting increased intensity can be observed along the coast at time step distance $4 - 5$.

However, the high-frequency representation (meaning the visualization of the low pyramid-level distance) is revealing the movement and development of critical point features. Figure 6 shows the difference between step one and step five, meaning the changes over five hours. It can be observed that the small center south of Florida is slowly moving towards the coast. The large center, previously south-west of the Bermuda Islands has moved a little in north-western direction and is located west of Bermuda after five hours. The movement of the saddle point also shows an interesting pattern, first along the coast, then moving west.

5 Conclusions

We have presented two methods for structure-based comparative visualization of 2D flow fields. Our first method uses an interactive pattern comparison based on flow moment invariants to observe the evolution of certain flow patterns over time. We have demonstrated that this method can be used to track the flow patterns and observed movement, changes in size and orientation. The second contribution is the generation of difference images of the moment invariant space. This has been done for two levels of the flow moment pyramid to observe different scale frequencies. We have presented different metrics to reduce the multi-dimensional complex-valued data. We have studied one metric in in detail and have shown that this representation can be used to track critical flow behavior over time.
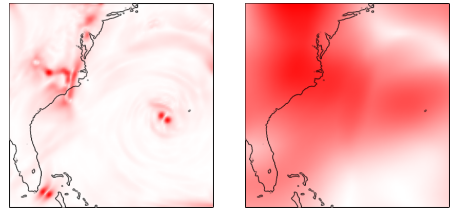

Figure 6: Moment pyramid comparison with distance between time step one and time step five for the first pyramid level (left) and the medium pyramid level (right).

References

[1] Steven P. Callahan, Juliana Freire, Emanuele Santos, Carlos E. Scheidegger, Cláudio T. Silva, and Huy T. Vo. Vistrails: visualization meets data management. In *SIGMOD '06: Proceedings of the 2006 ACM SIGMOD international conference on Management of data*, pages 745–747, New York, NY, USA, 2006. ACM.

[2] Julia Ebling and Gerik Scheuermann. Clifford convolution and pattern matching on vector fields. In Greg Turk, Jarke J. van Wijk,
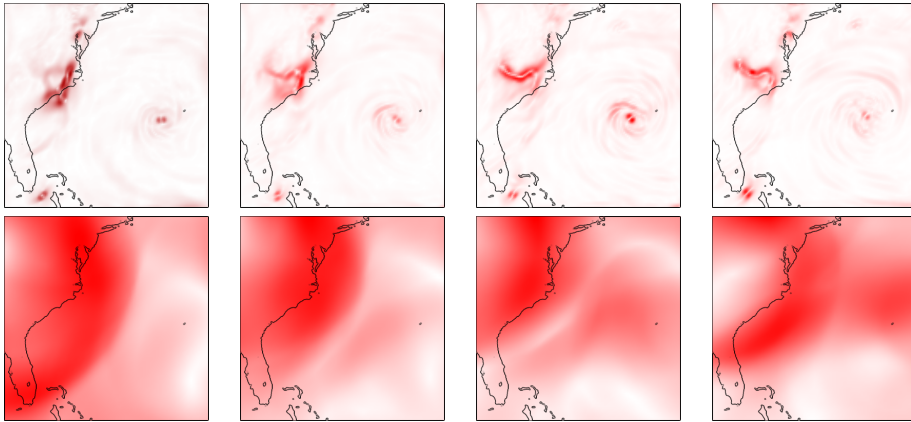
Figure 5: Moment pyramid comparison for different time steps of Hurricane Isabel. Distances on level one (high-frequency changes) are visualized in the upper row for similarity-distances between the time steps 1-2, 2-3, 3-4, and 4-5. In the row below, a higher level (half the pyramid's height) distance is visualized for the same time steps (indicating low-frequency changes).

and Robert Moorhead, editors, *Proceedings of IEEE Visualization 2003*, pages 193–200, Los Alamitos, CA, USA, 2003. IEEE Computer Society Press.

[3] Jan Flusser. On the independence of rotation moment invariants. *Pattern Recognition*, 33(9):1405–1410, 2000.

[4] Bernd Hentschel, Christian Bischof, and Torsten Kuhlen. Comparative visualization of human nasal airflows. *Stud Health Technol Inform*, 125:170–5, 2007.

[5] Ming-Kuei Hu. Visual pattern recognition by moment invariants. *IRE Transactions on Information Theory*, 8(2):179–187, February 1962.

[6] Suresh K. Lodha, Alex Pang, Robert E. Sheehan, and Craig M. Wittenbrink. UFLOW: Visualizing uncertainty in fluid flow. In Roni Yagel and Gregory M. Nielson, editors, *IEEE Visualization '96,*, pages 249–254, 1996.

[7] Hans-Georg Pagendarm and Frits H. Post. Studies in comparative visualization of flow features. In *Scientific Visualization, Overviews, Methodologies, and Techniques*, pages 211–227, Washington, DC, USA, 1997. IEEE Computer Society.

[8] Hans-Georg Pagendarm and Birgit Walter. Competent, compact, comparative visualization of a vortical flow field. *IEEE Transac-*

tions on Visualization and Computer Graphics, 1(2):142–150, 1995.

[9] Tobias Salzbrunn, Heike Jänicke, Thomas Wischgoll, and Gerik Scheuermann. The state of the art in flow visualization: Partition-based techniques. In *Simulation and Visualization 2008 Proceedings*, 2008.

[10] Michael Schlemmer, Manuel Heringer, Florian Morr, Ingrid Hotz, Martin Hering-Bertram, Christoph Garth, Wolfgang Kollmann, Bernd Hamann, and Hans Hagen. Moment invariants for the analysis of 2d flow fields. *IEEE Transactions on Visualization and Computer Graphics (Proceedings IEEE Visualization 2007)*, 13(6):1743–1750, nov 2007.

[11] Nikolai A. Svakhine, Yun Jang, David Ebert, and Kelly Gaither. Illustration and Photography Inspired Visualization of Flows and Volumes. In *IEEE Visualization 2005*, 2005.

[12] Vivek Verma and Alex Pang. Comparative flow visualization. *IEEE Transactions on Visualization and Computer Graphics*, 10(6):609–624, 2004.